A COMBUSTION MODEL TO PREDICT LOCAL EXTINCTION OF PARTIALLY PREMIXED FLAMES

Benjamin T. Zoller*, Patrick Jenny*
zoller@ifd.mavt.ethz.ch
*Institut of Fluid Dynamics, ETH Zurich, Sonneggstr. 3, 8092 Zurich

Abstract

A model to predict local extinction of partially premixed flames is presented. The new approach is based on parametrized scalar profiles (PSP) and can be viewed as a generalization of the PSP mixing model. It was demonstrated earlier that the PSP model can accurately predict joint distributions of multiple inert scalars and corresponding scalar dissipation rates. Here, the profile parametrization is generalized for reactive scalars. For this purpose a flammable range on the profile is considered. There, the chemical state is set to that in a laminar flamelet solution. The chemical states of the particles employed by a PDF solution algorithm relax towards the parametrized reactive profiles, whereas the position in such a profile is determined by the mixture fraction; latter is governed by the non-reactive PSP model. To account for flame propagation, an ignition probability model is employed, which determines the mean concentration of burning profiles. To test this approach, simulations of the Sandia D and F flame employing the same model parameters were conducted. The PDF results of the Sandia D and F flame with a largely different degree of local extinction are in good agreement with the measurements.

Introduction

As around 80% of the global energy consumption is covered by burning fuels [1], there exists a great interest in the development of improved combustion devices. For many such devices save operation conditions are of prime importance and therefore reliable prediction of local and global extinction is vital. Latter is a challenging modeling task, for which different approaches have been suggested.

Transported probability density function (PDF) methods [2, 3, 4] are attractive for turbulent reactive flow simulations as they allow to process valuable joint statistical information and thus can help to circumvent some of the critical closure problems, of which other approaches are suffering. Originally the main motivation for PDF methods was their advantage that the closure problem of averaging non-linear reaction source terms can be avoided, since the joint distribution of species mass fractions and temperature is available. One ansatz is based on direct integration of a detailed (e.g. [5]) or a reduced chemical mechanism [6, 7]. A problem there is the typically huge computational cost, even if it is dramatically reduced with advanced tabulation techniques like the ISAT algorithm [8], it remains high [9]. A more fundamental modeling problem is modeling of molecular mixing, which is crucial for turbulent combustion simulations. In fact, if direct integration or ISAT is applied, global extinction is subject to a "competition" between chemical reactions and molecular mixing, and the quality of the micro-mixing model is decisive. Moreover, it is problematic to treat mixing and reactions in two separate steps. For example, a mixing model has to account for the steepening of reactive scalar gradients due to chemical reactions; therefore in some cases the mechanical-to-scalar time scale ratio is increased (e.g. in [10]). Alternative approaches include various mapping closures like the widely used flamelet approach [11, 6], the multi moment closure (MMC) [12] or the REDIM approach [13]. However, all these models rely on stable chemical reactions and therefore, at

least in their basic form, they are unsuited to predict extinction. To close this gap between the flamelet at the quenching limit and the limit of pure diffusion, several methods to extend the flamelet approach have been proposed [14, 15, 16, 17, 18].

The method devised in this paper is based on a reactive PSP (R-PSP) model combined with a progress variable. The R-PSP model relies on parameterizations of burning and non-burning scalar profiles. While the previously developed PSP model [19] is employed for the non-reacting scalars (mixture fraction and reactive scalars of non-burning profiles), a more general parametrization is required for the burning scalar profiles. Therefore, in addition to the profile length and boundary compositions, also the chemical state in the enclosed reaction zone, which is obtained from a flamelet library conditional on the local scalar dissipation rate, is taken into account. Here it is assumed that "ignition" of a non-burning profile occurs due to flame propagation and that such a profile is "ignitable" only if it overlaps with the flammable mixture fraction range and if the scalar-dissipation rate in the flammable range is below the quenching limit. To describe "ignition", an "ignition" probability is introduced and has to be modeled.

A similar PDF method with the R-PSP mixing model and a closure for the "ignition" probability was already successfully applied by Hegetschweiler et al. [20] to predict stationary solutions of the Sandia F flame. In this paper it could be shown that the R-PSP model accurately predicts the Sandia D and F flame with the same model constants applied.

In the next two sections, a brief overview of the PDF approach and the PSP mixing model for inert scalars is given. Then, the R-PSP model is introduced and closure of the "ignition" probability is discussed. Finally, validation studies are presented before the paper is concluded.

PDF Modeling Framework

Before the combustion model is explained, we describe the probability density function (PDF) modeling [2] framework which is used here. The transport equation for the mass weighted joint PDF $f(\boldsymbol{V}, \theta, \boldsymbol{\Psi}; \boldsymbol{x}, t)$ of velocity $\boldsymbol{U}$, turbulence frequency ω and scalar vector $\boldsymbol{\phi}$ in physical space $\boldsymbol{x}$ and time t reads

$$\begin{aligned} \frac{\partial \langle\rho\rangle f}{\partial t} &+ \frac{\partial}{\partial x_j}\left(V_j \langle\rho\rangle f\right) \\ &- \frac{\partial}{\partial V_j}\left(\left\langle \frac{1}{\rho}\frac{\partial p}{\partial x_j}\middle| \boldsymbol{V}, \theta, \boldsymbol{\Psi}; \boldsymbol{x}, t\right\rangle \langle\rho\rangle f\right) + \frac{\partial}{\partial V_j}\left(\left\langle \frac{1}{\rho}\frac{\partial \tau_{ij}}{\partial x_i}\middle| \boldsymbol{V}, \theta, \boldsymbol{\Psi}; \boldsymbol{x}, t\right\rangle \langle\rho\rangle f\right) \\ &+ \frac{\partial}{\partial \Psi_\alpha}\left(\left\langle \frac{\mathrm{D}\phi_\alpha}{\mathrm{D}t}\middle| \boldsymbol{V}, \theta, \boldsymbol{\Psi}; \boldsymbol{x}, t\right\rangle \langle\rho\rangle f\right) + \frac{\partial}{\partial \Theta}\left(\left\langle \frac{\mathrm{D}\omega}{\mathrm{D}t}\middle| \boldsymbol{V}, \theta, \boldsymbol{\Psi}; \boldsymbol{x}, t\right\rangle \langle\rho\rangle f\right) \\ &= \mathcal{S}(\langle\rho\rangle f)\,, \end{aligned} \tag{1}$$

where $\langle\cdot|\cdot\rangle$ and $\langle\cdot\rangle$ denote conditional and unconditional expectations. Furthermore, $\boldsymbol{V}$, θ and $\boldsymbol{\Psi}$ are the sample space variables of $\boldsymbol{U}$, ω and $\boldsymbol{\phi}$, respectively. Moreover, ρ is the density, p the pressure and τ_{ij} the viscous stress tensor. The last term accounts for jump processes, which may be considered for the evolution of certain scalars, e.g. of a binary progress variable as introduced later in this paper.

Due to the high dimensionality of the $\boldsymbol{V}$-θ-$\boldsymbol{\Psi}$-$\boldsymbol{x}$-space in which Eq. (1) has to be solved, typically particle Monte Carlo methods are employed to compute numerical solutions. The mass density function $\langle\rho\rangle f$ is then represented by a cloud of computational particles in the $\boldsymbol{V}$-θ-$\boldsymbol{\Psi}$-$\boldsymbol{x}$-space, which evolve in time according to stochastic differential equations (SDEs). These SDEs are constructed such that the particle cloud evolution is consistent with a modeled PDF transport equation. Here for example, particles (particle properties are denoted by the superscript $*$) with a weight m^*, position $\boldsymbol{x}^*$, velocity $\boldsymbol{U}^*$, a turbulence frequency ω^* and a particle property vector

$\boldsymbol{\phi}^*$ (required for the combustion model) evolve according to the equations

$$\frac{\mathrm{d}x_i^*}{\mathrm{d}t} = U_i^* \,, \tag{2}$$

$$\begin{aligned} \mathrm{d}U_i^* &= \left[-\frac{1}{\langle\rho\rangle}\frac{\partial\langle p\rangle}{\partial x_i} + \frac{1}{\langle\rho\rangle}\frac{\partial\left\langle\tau_{ij}\right\rangle}{\partial x_j} - \left(\frac{1}{2}+\frac{3}{4}C_0\right)\Omega\left(U_i^* - \widetilde{U_i}\right)\right]\mathrm{d}t \\ &+ \sqrt{C_0 k\Omega}\,\mathrm{dW}_i \quad \text{and} \end{aligned} \tag{3}$$

$$\begin{aligned} \mathrm{d}\omega^* &= \left[-C_3\left(\omega^* - \widetilde{\omega}\right)\Omega - \left(C_{\omega 2} - C_{\omega 1}\frac{P}{k\Omega}\right)\Omega\omega^*\right]\mathrm{d}t \\ &+ \sqrt{2C_3C_4\widetilde{\omega}\Omega\omega^*}\,\mathrm{dW}_\omega \,, \end{aligned} \tag{4}$$

where $P = -\widetilde{u_i u_j}\partial\widetilde{U_i}\partial x_j$ is the turbulence production term, $k = \widetilde{u_j u_j}/2$ the turbulent kinetic energy and Ω the conditional turbulence frequency, which is employed to account for intermittency effects as suggested by Jayesh and Pope (found in [3]). The operator $\widetilde{\cdot}$ denotes mass (or Favre) averaged quantities, C_0, $C_{\omega 1}$, $C_{\omega 2}$, C_3 and C_4 are model constants and W_i is a Wiener process ($\mathrm{dW_i}$ has a normal distribution with $\langle \mathrm{dW_i}\rangle \equiv 0$ and $\left\langle \mathrm{dW}_i\mathrm{dW}_j\right\rangle = \mathrm{d}t\,\delta_{ij}$). For the velocity equation (3), the simplified Langevin model (SLM) [3] was employed to close the fluctuating viscous and pressure terms, and Eq. (4) represents the Gamma distribution model for the turbulence frequency. If compressibility effects are neglected (low Mach numbers), then the mean pressure $\langle p\rangle$ can be computed on a grid by solving the Reynolds averaged Poisson equation

$$\frac{\partial^2\langle p\rangle}{\partial x_i\partial x_i} = \frac{\partial^2\langle\rho\rangle}{\partial t\partial t} + \frac{\partial^2}{\partial x_i\partial x_j}\left[\left\langle\tau_{ij}\right\rangle - \langle\rho\rangle\left(\widetilde{U}_i\widetilde{U}_j + \widetilde{u_i u_j}\right)\right] \,, \tag{5}$$

in which the first right-hand side term can be ignored, if only steady state solutions are considered. All averaged quantities in Eqs. (3), (4) and (5) can be estimated from the particle cloud, e.g. first extracted at the nodes of the grid employed to solve (5) and then interpolated from there to the particle positions. A detailed description of a similar algorithm is found in [21], where also a more efficient, consistent hybrid finite volume/particle PDF solution algorithm is described. Latter was also employed for this work.

Short Review of the PSP Mixing Model

In the present work, the PSP mixing model by Meyer and Jenny [19, 22, 23] is employed to evolve the mixture fraction values $Z^* = \phi_1^*$ (here the first component of the scalar vector $\boldsymbol{\phi}^*$). In the PSP mixing model the turbulent scalar field is represented by embedded scalar profiles (1D, but aligned with the local scalar gradient). With this assumption, the scalar evolution is governed by the one dimensional diffusion equation for constant diffusity and density along the profile

$$\frac{dZ^*}{dt} = \Gamma_Z^*\left[\frac{\partial^2 Z'}{\partial x'\partial x'}\right]_{Z'=Z^*} \,, \tag{6}$$

where Γ_Z^* is the diffusion coefficient of the mixture fraction on the profile, x' a local space coordinate along the scalar gradient and $Z'(x',t)$ the parametrized mixture fraction profile. For

the parametrization at a given instance t, the sinusoidal ansatz

$$Z'(x',t) = \underbrace{\frac{Z^{*,+} - Z^{*,-}}{2}}_{Z^{*,a}} \sin\left(\frac{x'\pi}{\lambda^*}\right) + \underbrace{\frac{Z^{*,+} + Z^{*,-}}{2}}_{Z^{*,c}} \quad \text{with } x' \in [-\lambda^*/2, \lambda^*/2] \tag{7}$$

is used, which then is employed to close the right-hand side of Eq. (6) leading to

$$\frac{dZ^*}{dt} = -\underbrace{\Gamma_Z^* \left(\frac{\pi}{\lambda^*}\right)^2}_{C'_\phi \omega^*/2 = 1/\tau_\phi^*} (Z' - Z^{*,c})_{Z'=Z^*} = -\frac{1}{\tau_\phi^*}(Z^* - Z^{*,c}) \,. \tag{8}$$

Note that the profile length λ^* is related to the mixing time scale τ_ϕ^* as $\lambda^* = (\Gamma_Z^* \pi^2 \tau_\phi^*)^{1/2}$, and according to Spalding's suggestion of a constant mechanical to scalar time scale ratio, a constant value for C'_ϕ is employed. Note that formulation (8) is similar to the IEM mixing model, except that the mixing time scale τ_ϕ^* and the drift target $Z^{*,c}$ are modeled individually for each computational particle; in the IEM model, $2/(C_\phi \widetilde{\omega})$ and $\widetilde{Z}$ are used instead of τ_ϕ^* and $Z^{*,c}$, respectively. Figure 1 shows an illustration of a parametrized mixture fraction profile.

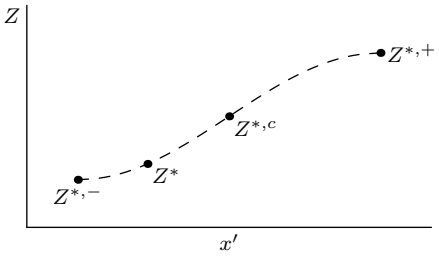

Figure 1: Illustration of parametrized inert scalar profile.

In a turbulent flow field, the profile boundary values $Z^{*,\pm}$ themselves evolve and have to be updated every time step. On one hand, they are re-initialized periodically when either the constraint $Z^{*,-} \leq Z^* \leq Z^{*,+}$ gets violated or when the lifetime of a profile is over. At each re-initialization event the $Z^{*,\pm}$ values are set equal to the mixture fractions of two arbitrary particles from the same ensemble and the new lifetime is set proportional to $1/\omega^*$ [19]. On the other hand, between two re-initialization events $Z^{*,\pm}$ evolve continuously, for which several submodels have been suggested [19, 22, 23]. In this work we employ the IEM boundary treatment, in which the profile boundary values drift towards the mean value like

$$\frac{\mathrm{d}Z^{*,\pm}}{\mathrm{d}t} = -\frac{1}{2} C''_\phi \widetilde{\omega} \left(Z^{*,\pm} - \widetilde{Z}\right) \,, \tag{9}$$

where C''_ϕ is a further model constant.

The PSP mixing model is particularly suited for flamelet modeling, as the instantaneous scalar dissipation rates can be obtained accurately from the parametrized fine-scale profile [22, 23], e.g. for the mixture fraction Z

$$\chi_Z^*(Z) \equiv 2\Gamma_Z^* \left[\frac{\partial Z'}{\partial x_j}\frac{\partial Z'}{\partial x_j}\right]_{Z'=Z} = C'_\phi \omega^* \left(Z^{*,+} - Z\right)\left(Z - Z^{*,-}\right) \,. \tag{10}$$

Reactive PSP Model

In the case of reactive scalars the assumption of self-similar sinusoidal profiles is not justified and therefore a more general parametrization is required. Here a reactive PSP (R-PSP) model is devised, in which both molecular mixing and chemical reactions of multiple scalars (one of them an inert mixture fraction) are treated together. While the PSP model for inert scalars is employed to evolve the mixture fraction, evolving the reactive scalars is more complicated. For the following explanations we consider the sensible enthalpy h as the reactive scalar of interest and discuss profiles in the Z-h-space. Similar as in the steady flamelet approach, it is assumed for a burning profile that the chemical state within the flammable mixture fraction range is in reactive-diffusive equilibrium. This equilibrium depends on the scalar dissipation rate of Z close to the stoichiometric value Z^{st}; like the flammable mixture fraction range $[Z^{st,-}, Z^{st,+}]$. Now, together with the profile boundary values $(Z,h)^{*,\pm}$ one can construct a burning profile in the Z-h-space. Next, for simplicity and clarity the profile construction is explained for the Burke-Schumann limit, i.e. $Z^{st} = Z^{st,-} = Z^{st,+}$.

As already mentioned, it has to be distinguished between burning and non-burning profiles. A profile is considered burning, if the requirement

$$Z^{*-} \leq Z^{st} \leq Z^{*,+} \quad \wedge \quad \chi_Z^*(Z^{st}) < \chi_Z^q \quad \wedge \quad c^* = 1 \tag{11}$$

is met, where χ_Z^q is the quenching limit and $c^* \in \{0,1\}$ a modeled progress variable indicating whether a profile is "ignited". With Eq. (10), condition (11) can be expressed as

$$0 \leq (Z^{*,+} - Z^{st})(Z^{st} - Z^{*,-})C'_\phi \omega^* < c^* \chi_Z^q \,. \tag{12}$$

Non-burning profiles are treated by the PSP model for inert scalars, i.e. in the Z-h-space the particle state $(Z,h)^*$ drifts straight towards the attraction point $(Z,h)^{*,a} = (Z,h)^{*,c}$ (see Figure 2). Moreover, at reinitialization two arbitrary particles from the same ensemble are selected to

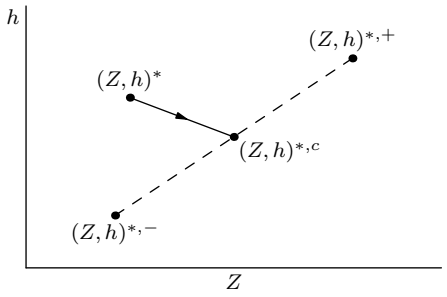

Figure 2: Parametrized non-burning profile in Z-h-space. Also shown is the particle state $(Z,h)^*$ and the relaxation direction towards the attraction point $(Z,h)^{*,c}$ (arrow).

determine the new profile boundary states.

In the case of burning profiles the parametrization consists of two connected lines in the Z-h-space, i.e. of a left branch connecting the point $(Z,h)^{*,-}$ with $(Z,h)^{*,st}$ and a right branch connecting $(Z,h)^{*,st}$ with $(Z,h)^{*,+}$. The first coordinate of the point $(Z,h)^{*,c}$ is $Z^{*,c} = (Z^{*,-} + Z^{*,+})/2$, while

$$h^{*,c} = \begin{cases} h^{*,-} + \frac{h^{*,st} - h^{*,-}}{Z^{st} - Z^{*,-}}(Z^{*,c} - Z^{*,-}) & \text{if} \quad Z^{*,c} \leq Z^{st} \\ h^{*,st} + \frac{h^{*,+} - h^{*,st}}{Z^{*,+} - Z^{st}}(Z^{*,c} - Z^{st}) & \text{if} \quad Z^{*,c} > Z^{st} \,, \end{cases} \tag{13}$$

where $h^{*,st}$ is estimated from a laminar flamelet solution. Two such profiles are depicted in Figure 3. In the left one, Z^* and $Z^{*,c}$ are on the same side of Z^{st} (here both Z^* and $Z^{*,c}$ are smaller than Z^{st}) and the particle state $(Z,h)^*$ drifts straight towards the attraction point $(Z,h)^{*,a} = (Z,h)^{*,c}$ (the drift rate is dictated by the mixing of Z^*). In the profile of Figure 3(b) Z^* and $Z^{*,c}$ lie on opposite sides of Z^{st} (here $Z^* < Z^{st} < Z^{*,c}$). In such cases, to satisfy localness, the particle state $(Z,h)^*$ drifts straight towards the attraction point $(Z,h)^{*,a} = (Z,h)^{*,st}$ (again the drift rate is dictated by the mixing of Z^*). More formally, the enthalpy change Δh^* of a particle

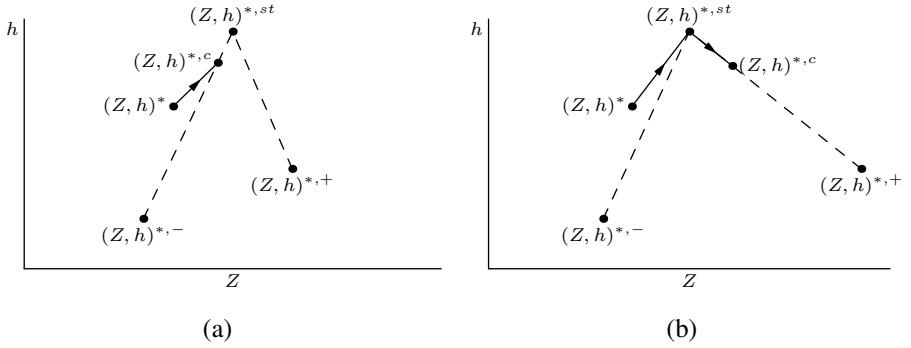

Figure 3: Parametrized burning profiles in the Z-h-space (Burke-Schumann limit). Also shown are particle states $(Z,h)^*$ and relaxation directions towards the attraction points (arrows).

during one time step of size Δt can be written as

$$\Delta h^* = \frac{h^{*,a} - h^*}{Z^{*,a} - Z^*} \Delta Z^* \,, \tag{14}$$

where ΔZ^* is the change of Z^* governed by the PSP mixing model for inert scalars. To determine the new boundary states, $Z^{*,\pm}$ and reactive scalars of non-burning profiles are treated like in the PSP model for inert scalars, while for burning profiles the reactive scalars at the profile boundaries are set to the corresponding flamelet solution.

So far the Burke Schumann limit was considered. Now it is explained how this model can be generalized for more realistic cases with finite rate chemistry. For this extension it has to be considered that reactions not only occur under stoichiometric conditions, but rather within a flammable range, where $Z \in [Z^{st,-}, Z^{st,+}]$ with $Z^{st,-} < Z^{st} < Z^{st,+}$. To account therefore, Z^{st} in the R-PSP model explained above is replaced by the uniformly distributed random variable $\hat{Z}^{*,st} \in [Z^{st,-}, Z^{st,+}] \cap [Z^{*,-}, Z^{*,+}]$. More difficult to treat are the secondary reactions, which occur outside of the defined range $[Z^{st,-}, Z^{st,+}]$ and as a result the particle states do not drift on a straight line towards the attraction points. To account for this non-linear relaxation, a simple mapping was introduced to the model. Therefore the sensible enthalpy is expressed as

$$h^* = h^{*,cold} + a^*(h^{*,flamelet} - h^{*,cold}) \,, \tag{15}$$

where $h^{*,flamelet} = h^{flamelet}(Z^*, \chi^*)$ and $h^{*,cold} = h^{cold}(Z^*)$ are the enthalpies from the reacting and non-reacting flamelet solutions, respectively, and $a^* = (h^* - h^{*,cold})/(h^{*,lamelet} - h^{*,cold})$. Now, to compute the evolution of h^*, one has to replace Eq. (14) with

$$\Delta a^* = \frac{a^{*,a} - a^*}{Z^{*,a} - Z^*} \Delta Z^* \,. \tag{16}$$

Local extinction of partially premixed flames is mainly governed by quenching, i.e. it occurs where the scalar dissipation rate (of the mixture fraction in the flammable range) exceeds the quenching limit. It is assumed here that re-ignition of a non-burning, but ignitable profile occurs due to embedded triple flames propagating along stoichiometric mixture fraction manifolds and that re-ignition is only possible, if the scalar dissipation rate is below the quenching limit; an illustrative sketch (motivated by DNS data by Domingo and Vervisch [24]) is shown in Figure 4 (note that autoignition is not considered in this work). In general there exists a competition of embedded triple flame propagation against local extinction and flow velocity. In the presented model, as already mentioned at the beginning of this section, the state of a profiles is either burning (if $c^* = 1$) or non-burning (if $c^* = 0$); the non-burning profiles represent states in front and the burning ones states behind the triple flame tips. While it is straight forward to

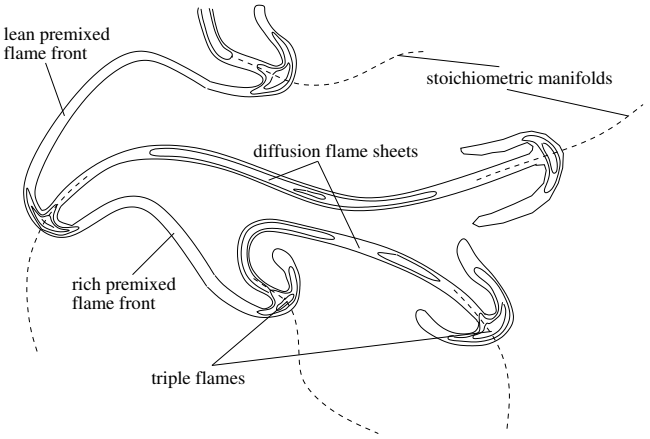

Figure 4: Sketch of quasi laminar triple flames propagating along stoichiometric manifolds into the fresh gas embedded in a turbulent flow field (inspired by Domingo and Vervisch [24]).

model local extinction, since the PSP model automatically delivers local scalar dissipation rates, dealing with re-ignition is more tricky. Therefore the "ignition" probability P was introduced, which quantifies the likelihood that an ignitable (but non-burning) profile is "reached" by a triple flame during a time step of size Δt. Here the model ansatz

$$P = 1 - \exp\left(-\beta_2 \tilde{\omega} \langle c \rangle^2 \triangle t\right) \tag{17}$$

is proposed, where for this work β_2 is a constant. Note that P is zero for $\langle c \rangle = 0$ and rises monotonically with $\langle c \rangle$.

Parameters and Results

Validation studies were performed with the Sandia D and F flames. Both are axi-symmetric jet flames with a concentric pilot stream surrounded by an co-flow of 1 m/s. The jets consist of methane diluted with air and have a diameter of $d = 0.0072m$. The surrounding pilot stream is a premixed flame, for which we assume a mixture fraction to match an inlet temperature of $1880K$; following the mixture fraction definition used for the experiments [25]. The jet and pilot bulk velocities for Sandia D flame are $49.6m/s$ and $11.4m/s$, respectively; for the Sandia F flame they are $99.2m/s$ and $22.8m/s$. Further information about the experimental setup and the measurement techniques can be found on the web page of the International Workshop on Measurement and Computation of Turbulent Non-Premixed flames (TNF workshop) [25]. The flamelet library was produced with the FlameMaster code by Pitsch [26], whereas the widely

used GRI 2.11 mechanism was employed [5]. For the tabulation, 30 flamelet solutions for scalar dissipation rates ranging from $\chi_{\mathrm{st}} = 2.0$ to $\chi_{\mathrm{q}} = 400.0$ were employed.
For the PDF simulations, an axi-symmetric 2D code was used. The orthogonal grid has a size of 50 cells in axial and 60 cells in radial direction and is condensed in the jet and pilot regions. An average of approximately 50 particles per cell was enforced by a consistent particle number control algorithm. For the choice of the modeling parameters, the standard values of the SLM proposed by Jayesh and Pope were used; expect for the constant $C_{\omega 1}$, which was adjusted to 0.75. For the mixing model constants C'_ϕ and C_t the suggested values of Meyer and Jenny [22] were employed, i.e. $C'_\phi = 13$ and $C_t = 13$, and C''_ϕ was set to 2.5. However, as demonstrated in [20], the results are quite insensitive to the choice of these mixing model constants. The constant β_2 was employed to "tune" the Sandia F flame results, but then the same value of 100 was employed for the Sandia D flame calculations. Finally, the flammable range was set to $[Z^{st,-} = 0.1, Z^{st,+} = 0.6]$.

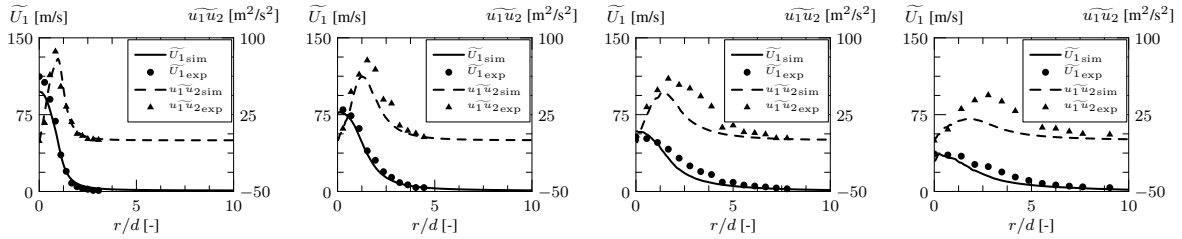

(a) $x/d = 15$ (b) $x/d = 30$ (c) $x/d = 45$ (d) $x/d = 60$

Figure 5: Sandia F flame results of mean axial velocity ($\widetilde{U_{1\mathrm{sim}}}$) and covariance ($\widetilde{u_1u_{2\mathrm{sim}}}$) in comparison with experimental data ($\widetilde{U_{1\mathrm{exp}}}$, $\widetilde{u_1u_{2\mathrm{exp}}}$) at various downstream positions.

First, the results of the Sandia F flame are presented together with the experimental data. Figure 5 shows the mean axial velocity $\widetilde{U_1}$ and the Reynolds stress $\widetilde{u_1u_2}$. The radial profiles of $\widetilde{U_1}$ are predicted very well; the covariance $\widetilde{u_1u_2}$ on the other hand is under-predicted downstream of $x/d = 45$. A possible explanation for this under-prediction might be that the relaminarization which takes place far downstream can not accurately be captured by the SLM.
Figures 6 and 7 depict radial profiles of mean mixture fraction $\widetilde{Z}$ and temperature $\widetilde{T}$ together

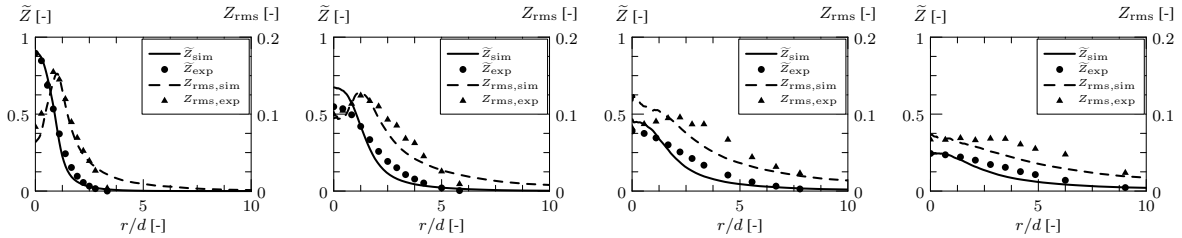

(a) $x/d = 15$ (b) $x/d = 30$ (c) $x/d = 45$ (d) $x/d = 60$

Figure 6: Sandia F flame results of mean mixture fraction ($\widetilde{Z}_{\mathrm{sim}}$) and its rms value ($Z_{\mathrm{rms,sim}}$) in comparison with experimental data ($\widetilde{Z}_{\mathrm{exp}}$, $Z_{\mathrm{rms,exp}}$) at various downstream positions.

with their rms values. While $\widetilde{Z}$ is slightly over-predicted along the symmetry axis, the rms

values of Z generally are in good agreement, except the location of the peak is a bit off at the downstream positions $x/d = 45$. Also the radial mean temperature profiles are in good agreement; the rms temperature is generally under-predicted.

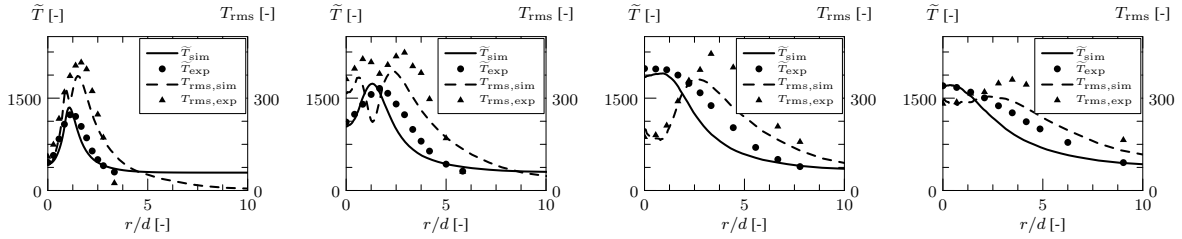

(a) $x/d = 15$ (b) $x/d = 30$ (c) $x/d = 45$ (d) $x/d = 60$

Figure 7: Sandia F flame results of mean mixture temperature ($\widetilde{T}_{\mathrm{sim}}$) and its rms value ($T_{\mathrm{rms,sim}}$) in comparison with experimental data ($\widetilde{T}_{\mathrm{exp}}$, $T_{\mathrm{rms,exp}}$) at various downstream positions.

Below the results for the Sandia D flame calculations are presented. In Figure 8 the mean axial velocity $\widetilde{U_1}$ and its covariance $\widetilde{u_1 u_2}$ are shown. Like in the Sandia F flame calculations, the radial profiles of $\widetilde{U_1}$ are predicted well, except for a small over-prediction downstream of the position $x/d = 45$, but the covariance $\widetilde{u_1 u_2}$ is under-predicted. Again it is speculated that latter inaccuracy might be due to the inability of the SLM to capture relaminarization effects, which are more pronounced in this test case.

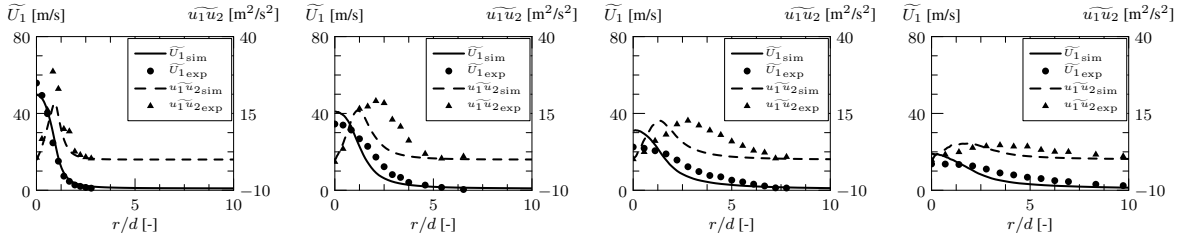

(a) $x/d = 15$ (b) $x/d = 30$ (c) $x/d = 45$ (d) $x/d = 60$

Figure 8: Sandia D flame results of mean axial velocity ($\widetilde{U_{1\mathrm{sim}}}$) and covariance ($\widetilde{u_1 u_{2\mathrm{sim}}}$) in comparison with experimental data ($\widetilde{U_{1\mathrm{exp}}}$, $\widetilde{u_1 u_{2\mathrm{exp}}}$) at various downstream positions.

Figures 9 and 10 depict radial and axial profiles of mean mixture fraction $\widetilde{Z}$ and temperature $\widetilde{T}$ together with their rms values. Overall mean and rms mixture fraction values are predicted well, except for the over-prediction of $\widetilde{Z}$ around the symmetry axis and the under-prediction of Z_{rms} downstream of $x/d = 45$. Similarly good results can be observed for the radial mean and rms temperature profiles, despite at position $x/d = 60$ where $\widetilde{T}$ is over-predicted around the symmetry axis.

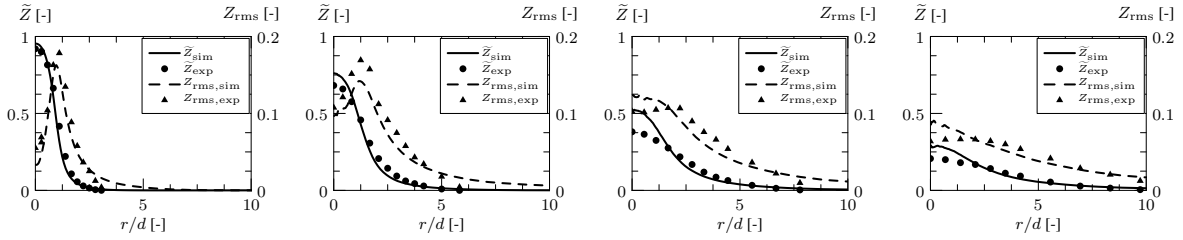

(a) $x/d = 15$ (b) $x/d = 30$ (c) $x/d = 45$ (d) $x/d = 60$

Figure 9: Sandia D flame results of mean mixture fraction ($\widetilde{Z}_{\mathrm{sim}}$) and its rms value ($Z_{\mathrm{rms,sim}}$) in comparison with experimental data ($\widetilde{Z}_{\mathrm{exp}}$, $Z_{\mathrm{rms,exp}}$) at various downstream positions.

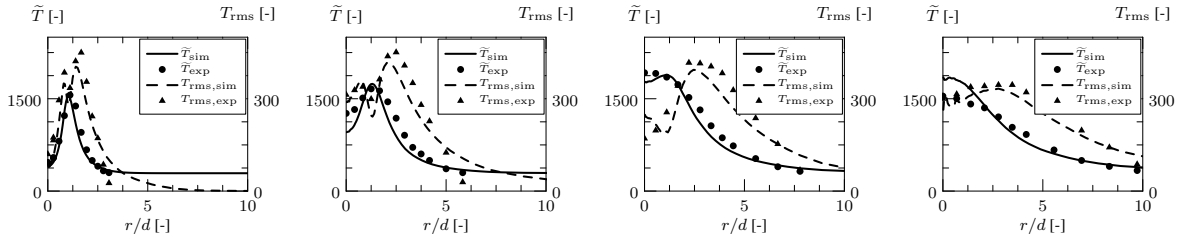

(a) $x/d = 15$ (b) $x/d = 30$ (c) $x/d = 45$ (d) $x/d = 60$

Figure 10: Sandia D flame results of mean temperature ($\widetilde{T}_{\mathrm{sim}}$) and its rms value ($T_{\mathrm{rms,sim}}$) in comparison with experimental data ($\widetilde{T}_{\mathrm{exp}}$, $T_{\mathrm{rms,exp}}$) at various downstream positions.

Conclusions

A model for partially premixed combustion in the context of transported PDF methods is devised, which extends the ideas of the inert PSP mixing model for reactive flows. To properly account for local extinction, two types of idealized reactive profiles are considered. Their states (burning or non-burning) evolve as function of their instantaneous scalar dissipation rates, the individual profile boundary conditions and an ignition probability; latter is decisive for re-igniting extinct profiles. Dependent on the profile state different profile parameterizations are employed; one for non-burning profiles like considered in the PSP model for inert scalars, and one for burning profiles, which involves an additional attraction point within the flammable range. The chemical state at the attraction point is taken from a corresponding laminar flamelet table.

Overall, studies of the Sandia flames D and F show good agreement between simulation results and experimental data. They also demonstrate that the model is capable of predicting two different jet flames with largely different degrees of local extinction.

As next step it is planned to investigate the capability of this model to predict global extinction. Therefore it will be necessary to better understand and improve the ignition probability model, which proved to be not very critical for the test cases presented in this paper. Furthermore it is intended to develop a mapping closure for the chemical state with additional progress variables to capture the ignition delay, which is neglected in the current version of the model.

[1] IEA, *Key World Energy Statistics 2008*, IEA, 2008.

[2] Pope, S. B., PDF methods for turbulent reactive flows, *Progress in Energy and Combustion Science* 11 (2): 119 – 192 (1985).

[3] Pope, S. B., *Turbulent Flows*, Cambridge University Press, 2000.

[4] Haworth, D., Progress in probability density function methods for turbulent reacting flows, *Progress in Energy and Combustion Science* 36 (2): 168 – 259 (2010).

[5] Bowman, C. et al., http://www.me.berkeley.edu/gri_mech/, available online (1995).

[6] Peters, N., *Turbulent Combustion*, Cambridge University Press, 2000.

[7] Maas, U. and Pope, S., Simplifying chemical kinetics: Intrinsic low-dimensional manifolds in composition space, *Combustion and Flame* 88 (3-4): 239 – 264 (1992).

[8] Pope, S. B., Compuationally efficient implementation of combustion chemistry using in situ adaptive tabulation, *Combustion Theory and Modelling* 1 (1): 41–63 (1997).

[9] Wang, H. and Chen, Y., PDF modelling of turbulent non-premixed combustion with detailed chemistry, *Chemical Engineering Science* 59 (16): 3477–3490 (2004).

[10] Raman, V., Fox, R. O. and Harvey, A. D., Hybrid finite-volume/transported PDF simulations of a partially premixed methane-air flame, *Combustion and Flame* 136 (3): 327 – 350 (2004).

[11] Peters, N., Laminar flamelet concepts in turbulent combustion, *Proceedings of the Twenty-First Symposuim (International) on Combustion* 21 (1): 1231 – 1250 (1988).

[12] Kronenburg, A. and Cleary, M., Multiple mapping conditioning for flames with partial premixing, *Combustion and Flame* 155 (1-2): 215 – 231 (2008).

[13] Bykov, V. and Maas, U., Problem adapted reduced models based on reaction-diffusion manifolds (REDIMs), *Proceedings of the Combustion Institute* 32 (1): 561 – 568 (2009).

[14] Pitsch, H., Chen, M. and Peters, N., Unsteady flamelet modeling of turbulent hydrogen-air diffusion flames, *Proceedings of the Twenty-Seventh Symposium (International) on Combustion* 1 - 2: 1057–1064 (1998).

[15] Pitsch, H., Cha, C. M. and Fedotov, S., Flamelet modelling of non-premixed turbulent combustion with local extinction and re-ignition, *Combustion Theory and Modelling* 7 (2): 317–332 (2003).

[16] Mitarai, S., Kosly, G. and Riley, J. J., A new lagrangian flamelet model for local flame extinction and reignition, *Combustion and Flame* 137 (3): 306–319 (2004).

[17] Pierce, C. and Moin, P., Progress-variable approach for large-eddy simulation of non-premixed turbulent combustion, *Journal of Fluid Mechanics* 504: 73–97 (2004).

[18] Ihme, M., Cha, C. M. and Pitsch, H., Prediction of local extinction and re-ignition effects in non-premixed turbulent combustion using a flamelet/progress variable approach, *Proceedings of the Combustion Institute* 30 (1): 793–800 (2005).

[19] Meyer, D. W. and Jenny, P., A mixing model for turbulent flows based on parameterized scalar profiles, *Phys. Fluids* 18 (3): 035105–15 (2006).

[20] Hegetschweiler, M., Zoller, B. T. and Jenny, P., Reactive parametrized scalar profiles (PSP) mixing model for partially premixed combustion, *submitted to Combustion and Flame*.

[21] Jenny, P., Pope, S. B., Muradoglu, M. and Caughey, D. A., A hybrid algorithm for the joint PDF equation of turbulent reactive flows, *Journal of Computational Physics* 166 (2): 218–252 (2001).

[22] Meyer, D. W. and Jenny, P., An improved mixing model providing joint statistics of scalar and scalar dissipation, *Combustion and Flame* 155 (3): 490 – 508 (2008).

[23] Meyer, D. W. and Jenny, P., A mixing model providing joint statistics of scalar and scalar dissipation rate, *Proceedings of the Combustion Institute* 32 (1): 1613 – 1620 (2009).

[24] Domingo, P. and Vervisch, L., Triple flames and partially premixed combustion in autoignition of non-premixed turbulent mixtures, *Symposium (International) on Combustion* 26 (1): 233 – 240 (1996).

[25] Barlow, R., http://www.ca.sandia.gov/TNF, TNF Workshop, available online.

[26] Pitsch, H., Flamemaster, A C++ computer program for 0D combustion and 1D laminar flame calculations.